Many-body physics of interacting bosons in optical lattice

A Synopsis (Approx. 5000 words)

Submitted by

Rhombik Roy

Under the supervision of

Dr. Barnali Chakrabarti

In partial fulfillment for the award of degree of

DOCTOR OF PHILOSOPHY

Department of Physics

Presidency University

Kolkata

Registration no. – R-17RS09120091

Date of Registration – 04/12/2018

Email: rhombikk@gmail.com

1 Introduction

Identical particles in quantum physics have statistical features that are radically different from those of their distinguishable classical counterparts since they cannot be distinguished. Bose originally brought this up in a derivation of Planck's law for photons [Bos24]. Then Einstein discovered [Ein25], particles with an integer spin, now known as bosons [Pau40], will gather in the energetic ground state under specific conditions and form a single coherent entity, called a Bose-Einstein condensate. This BEC plays the role as an initial start for all of the work discussed in this thesis. It took many years from the the time when the actual formation of a Bose-Einstein condensate (BEC) was made because of the necessity for advanced laser cooling techniques such as Doppler or Sisyphos cooling [HS75, NMCW95, CBZP92]. Finally, in 1995, three separate groups achieved success in independently lowering the temperature of a confined sample of ultracold bosons below the temperature threshold necessary for the production of BECs. A repulsive sodium was utilised by the first group, led by Ketterle [DMA+95], a repulsive rubidium by Cornell and Wieman [AEM+95], and an attracting lithium by Hulet [BSTH95]. There are several examples of physical systems where BECs can be employed as "quantum simulators," such as solid state devices [GME+02a]. Even greater class of physical systems can be studied in a highly controlled experimental setting because of the presence of contact and dipolar interparticle interactions in these samples. Recently, dipolar BECs in chromium [GWH+05] and dysprosium [LBYL11] have been realised. Besides, BEC has a wide range of application, for instance, in astrophysics [LIB+10], quantum computation [CDJ+04], study of BEC in optical lattice [MO06] etc. This is because the level of control that can be imposed on BECs in the lab is exceptional. The dimension of the system can be changed at any will [GVL+01, SKC+01]. Also, their constriction [HRMB09], and their interparticle interactions [CGJT10] can be changed nearly at whim. Because there are so many physical situations that can be easily accessed and managed, it is of great interest to investigate more fundamental many-body problems. Some of them I will discuss in this thesis.

Atoms must be tightly confined in two directions in order to form a 1D system of ultracold atoms. Optical lattices are one of the most commonly used methods for achieving such a high level of confinement [KWW04a, GBM+01]. To achieve this tight confinement, one of the most common technique is magnetic trapping. An atom is associated with a magnetic moment $\mu = g_F \mu_B F$, where F is the angular momentum, μ_B is the Bohr magneton and g_F is the Landé g-factor. If a weak magnetic field, B is applied, the Zeeman effect shifts atomic energy levels in a linear way. Now the magnetic field is varied slowly. As a result, the atoms will either be attracted to regions with lower magnetic fields or regions with higher magnetic fields. A purely magnetic trap can only hold low-field seeking states because Maxwell's equations forbid local maxima for static magnetic fields [SB97]. In order to get into the ultra-cold zone, evaporative cooling is a common method [DMJ+95]. In this procedure, a magnetic trap is used to confine an ensemble of particles that follow a Maxwell-Boltzmann velocity distribution. After that, the particles with the highest amount of energy will be the ones to break free of the trap, while those with a lower amount of energy will remain settled within it. The end result is a significant reduction in temperature, which is analogous to the process that causes coffee in a cup to become cooler. As a result, the particle loss rate increases, resulting in a condensate of the remaining particles.

Modern atomic physics study primarily focuses on quantum gases, which is one of the most exciting and rapidly developing topics. One of the most hotly debated topics in this subject is the investigation of ultracold quantum gases in optical lattices. When two or more laser beams interfere with one other, they create a standing wave of monochromatic light——a periodic intensity pattern generated by the interference of two or more laser beams. Atoms may be confined in areas of greatest or lowest intensity. Lasers of the same wavelength can be used to create the simplest feasible optical lattice. If additional laser beams are employed, one can create a periodic 3D crystal-like structure that mimics the crystal structure of a material in solid state physics. Experiments done in optical lattices provide numerous advantage: (1) By changing the intensity of the different optical lattice beams, the depth of the potential can be changed. By doing this, the way the atoms interact can also be changed. Also, the potential can be turned on and off and modified. This provides the system with unprecedented levels of control. (2) It is also possible to make lattice geometry like fcc, bcc crystal stricture. (3) In an optical lattice, the dimension of the quantum gas can be reduced from 3D to 1D or 2D easily.

The common mean-field method to describe the physics of interaction bosons in optical lattice is the Gross-Pitaevskii (GP) method. The wave-function is built from the product of a single orbital that has different spatial coordinates and has been appropriately normalised. Therefore, the GP equation is constructed on the premise that all bosons dwell in a single quantum state, which is precisely equal to the assertion that the bosons form a perfectly coherent condensate. Therefore, the TDGP model will be unable to adequately capture the dynamics and effects of first or higher order correlations, as well as first or higher order coherence or decoherence. Another very popular

method is the Bose Hubbard model which has two parameter: U controls the interaction between two atom and J is the hopping term between two lattice. But Its validity regime is limited to the situation where site-localized Wannier states are a suitable basis set. Thus Bose-Hubbard model fails to describe the physics in strong interaction regime. A description of the quantum many-body system that works for all kinds of interactions is the primary focus area and to slove the issue, I choose the multiconfigurational time-dependent Hartree method for bosons (MCTDHB) for my entire calculation. In this method, the many-body wave-function is written as the product of time dependent coefficient and time dependent orbitals which make the equation of motion variationally optimized quantity. The efficiency of MCTDHB is to make the sampled Hilbert space dynamically follow the time evolution of the many-body system. MCTDHB has been widely used in different theoretical calculations [RGT+18, RLL+19, RCT22] and results are very close to experimental predictions [LGK+21, NTL+19]. Detail discussion of MCTDHB method is given in sec 2.

In the course of my research for the doctoral degree, I have looked into a variety of systems, each of which has a specific interaction strength and potential, and I have done this for both time-dependent and time-independent scenarios. In our first study, we chose a $N = 3$ boson system loaded in a three-well optical lattice potential. A few bosons with contact interparticle interactions in optical lattices are known to exhibit a variety of quantum phases. Superfluid, Mott-insulator, and fermionized Tonks gases are among these quantum phases. All three phases were explored in my work by measuring the many-body Shannon information entropy, occupation in natural orbitals, and Glauber's normalised correlation measurements. In a separate study, we analysed the time dynamics of interacting bosons after a transition from small repulsive interaction to big repulsive interaction. Bosons are initially put into a shallow optical lattice. The phase transition occurs when the interaction strength is increased while the lattice depth remains constant. We examine the dynamical quantum phase transition between a superfluid phase and Mott-insulator. The Shannon information entropy, the occupation in natural orbitals, and the fidelity decay are the important measurements for this study. Our primary objective was to describe the relaxation processes by which the many observables of this quantum many-body system converge to equilibrium values over time. We have also worked on double well potential in a separate project. We quenched the optical trap while maintaining the interaction strength constant in order to examine the system's dynamics. Previously, we used variable contact interparticle interaction to explore the static or time development of a bosonic system. In this work, we choose long range interaction having the form $W(x_i - x_j) = \frac{g_d}{|x_i - x_j|^3 + \alpha_0}$. Where g_d is the strength of the interaction. Nature of this interaction is discussed in Sec.4.3. At this point, we set the system in an asymmetric double well potential and make the trap symmetric at a time of t equal to zero. We have extracted four distinct types of dynamics: (i) Josephson oscillation, (ii) deformed Josephson oscillation, (iii) self-trapping, and (iv) equilibrium. Measurement of population in each orbital, fragmentation dynamics, and two-body density measurements led us to this conclusion. In another work, we looked into the SDL and LMC measures of complexity for interacting bosons in the optical lattice. we like to track the path from the SF phase to the insulating phase by observing how order, disorder, and complexity change in the system. we find that different complexity structure makes it more sensitive than the traditional application of Shannon information entropy.

2 Methodology

We find the stationary solution of the many-body Schrödinger equation by MCTDHB implemented in the MCTDH-X software[LMP+20, Lod16, LLM+20] with periodic boundary condition. In MCTDHB, the wave-function of the interacting bosons is expanded over a set of permanents which are the symmetrized bosonic states of N bosons distributed over M single particle states.

$$|\Psi(t)\rangle = \sum_{\bar{n}} C_{\bar{n}}(t)|\bar{n};t\rangle, \tag{1}$$

The vector $\vec{n} = (n_1, n_2, \ldots, n_M)$ represent the occupation of the orbitals and $n_1 + n_2 + \ldots n_M = N$ preserve the total number of particle.

$$|\bar{n};t\rangle = \prod_{i=1}^{M} \left(\frac{\left(b_i^\dagger(t)\right)^{n_i}}{\sqrt{n_i!}} \right) |vac\rangle. \tag{2}$$

$b_k^\dagger(t)$ creates a boson occupying the time-dependent orbital $\phi_k(x,t)$. The number of possible configuration is $\begin{pmatrix} N+M-1 \\ N \end{pmatrix}$. It is important to note that both the expansion coefficients $(C_{\vec{n}}(t))$ and time dependent orbitals $(\phi_i(x,t))$ that build the permanents $|\vec{n},t\rangle$ are time dependent and fully variationally optimized quantities. Thus MCTDHB has been established as the most efficient way to solve the time dependent many-body Schrödinger

equation [ASC07, ASC08, LSA+12]. The efficiency of MCTDHB is to make the sampled Hilbert space dynamically follow the time evolution of the many-body system. MCTDHB has been widely used in different theoretical calculations [RGT+18, RLL+19, RCT22] and results are very close to experimental predictions [LGK+21, NTL+19]. For $M \to \infty$ limit, as the set of permanents $|\vec{n;t}\rangle$ span the complete Hilbert space, the expansion is exact. But during computation, we limit the size of the Hilbert space. As the permanents are now time dependent, a given degree of accuracy is achieved with the truncated basis as compared to time-independent basis. It is also proved that significant computational advantage is achieved over exact diagonalization [LCK15]. To solve the time dependent many-body Schrödinger equation $\hat{H}|\psi\rangle = i\frac{\partial|\psi\rangle}{\partial t}$ for the wave function $|\psi\rangle$, we calculate the time evolution of the coefficients $C_{\vec{n}}(t)$ and the orbitals $\phi_i(x,t)$. We utilize variational principle [Kva13, KS81] to obtain the equation of motion of the time dependent coefficient and orbital [ASC08, SAC07, ASC07, LB16]. Finally the coupled nonlinear integrodifferential equations are solved by MCTDHB package [LLM+20].

3 Quantity of interest

In this section, I will discuss the quantities that will be utilised in the process of solving the solutions of the Schrödinger equation. In order to investigate different phases or statistical relaxation, the measurements of different information entropies are utilised. The reduced one-body density in coordinate space defined as

$$\rho^{(1)}(x'|x;t) = N \int dx_2 dx_3 ... dx_N \psi^*(x', x_2, \ldots, x_N; t)\psi(x, x_2, \ldots, x_N; t). \tag{3}$$

Its diagonal ($x = x'$) gives the one-body density $\rho(x,t)$ as

$$\rho(x;t) = N \int dx_2 dx_3 ... dx_N \psi^*(x, x_2, \ldots, x_N; t)\psi(x, x_2, \ldots, x_N; t). \tag{4}$$

With the help of this equation, we will define the Shannon information entropy in coordinate space as

$$S_x(t) = -\int dx \rho^{(1)}(x,t) ln[\rho^{(1)}(x,t)]. \tag{5}$$

Similarly, the reduced one-body density in momentum space can be defined as

$$\rho^{(1)}(k'|k;t) = N \int dk_2 dk_3 ... dk_N \psi^*(k', k_2, \ldots, k_N; t)\psi(k, k_2, \ldots, k_N; t). \tag{6}$$

Its diagonal ($k = k'$) gives the one-body density $\rho(k,t)$ in momentum space defined as

$$\rho(k;t) = N \int dk_2 dk_3 ... dk_N \psi^*(k, k_2, \ldots, k_N; t)\psi(k, k_2, \ldots, k_N; t). \tag{7}$$

We make the density distribution normalized to unity. Even if there are correlations present in the many-body states, the one-body density is completely unaffected by them. This probe us to describe a different way of measuring many-body information in our calculation. As stated earlier, the many-body wave function in MCTDHB is written as $|\psi\rangle = \sum_{\vec{n}} C_{\vec{n}}(t)|\vec{n},t\rangle$. We define an alternative Shannon Information entropy using $C_{\vec{n}}$ as $C_{\vec{n}}$ describe the distribution of the state in the Fock space. We refer this entropy as coefficient Shannon information entropy and it is defined as

$$S_c(t) = -\sum_{\vec{n}} |C_{\vec{n}}(t)|^2 ln[|C_{\vec{n}}(t)|^2]. \tag{8}$$

For mean-field calculation, only one single orbital contributes in the formation of wave function. So, for this kind of calculation, $S_c = 0$ for all time. So, we cannot define coefficient Shannon information entropy for such mean-field calculation. Several expansion coefficients come into play whenever the state $|\psi\rangle$ spreads across several configurations $\vec{n};t\rangle$. Thus the coefficient Shannon information entropy (S_c) gradually increases. When the total N-body Fock space is populated by the state $|\psi\rangle$, the extreme situation, all the coefficients are of the same size and S_c saturates to its maximum value. This occurs when the state populates the entire space.
The emergence of fragmentation can be demonstrate by constructing a entropy measure which is associated with orbital occupation, i.e., the emergence of significant eigenvalues n_i of the reduced one-body density matrix. We term this entropy as occupational Shannon information entropy or orbital Shannon information entropy and it is defined as

$$S_n = -\sum_{i}^{M} n_i ln n_i \tag{9}$$

where the N particles are distributed over M orbitals: $N = n_1 + n_2 + \ldots n_M$. In the case of bosons, the reduced density matrix is defined by only a single eigenvalue, and as a result, $S_n = 0$ is true for the state that is described by a single-orbital mean-field theory. $S_n \neq 0$ for single-configuration states with multiple contributing orbitals as well as multiconfigurational states with multiple contributing orbitals. The occupation Shannon information entropy of the condensed gas is zero since there is only one occupation that dominates. When we increase the interaction strength, the same entropy steadily grows and saturates to the most fragmented state. It is thus possible to measure the dynamic fragmentation of the system using $S_n(t)$.

The next quantity of interest is the fidelity $F(t)$. It determines how much of the time-evolving wave function$|\psi(t)\rangle$ overlaps with the initial wave function $|\psi(t=0)\rangle$. The expression of fidelity is written as

$$F(t) = |\langle\psi(0)|\psi(t)\rangle|^2. \tag{10}$$

Because the analysis of the fidelity derived from an MCTDHB wave function needs the analysis of permanents, it can only be conducted for a limited number of particles. Fidelity is nothing but the modules square of auto-correlation function $c(t) = \langle\psi(0)|\psi(t)\rangle$. This auto-correlation function or the fidelity has a wide range of application in the field of molecular physics, many-body excitation spectra etc. The relationship between $c(t)$ and $F(t)$ shows that the time evolution of $F(t)$ is very sensitive to the many-body eigenstates and energies of the Hamiltonian.

The correlation function can also be used to explain coherence and fragmentation. To describe the correlation function, we first need to discuss about the p-body density and it can be represented as

$$\rho^{(p)}(x_1, x_2, \ldots, x_p) = \langle\psi|\hat{\psi}^\dagger(x_1)\ldots\hat{\psi}^\dagger(x_p)\hat{\psi}(x_p)\ldots\hat{\psi}(x_1)|\psi\rangle \tag{11}$$

where $\hat{\psi}^\dagger(x_i)$ is the creation operator at state x_i and $\hat{\psi}(x_i)$ is the annihilation operator. The diagonal part of the p-body density gives the probability to find p^{th} particle at x_p. The p^{th} order correlation function is defined as

$$g^{(p)}(x_1, x_2, \ldots, x_p) = \frac{\rho^{(p)}(x_1, x_2, \ldots, x_p)}{\Pi_{i=1}^{p}|\rho^{(1)}(x_i)|} \tag{12}$$

As long as the p-body density is made up of a single-body density, the system is completely coherent and $g^{(p)} = 1$ holds. When the p-body density is not a product of one-body densities, partial coherence can be achieved with $g^{(p)} \neq 1$. In my works, I have considered upto two-body correlation. In recent works, we are trying to implement higher order correlation function in our calculation.

The Shannon information entropy measures, order (Ω), disorder (Δ), and complexity are all part of the general information-theoretical measure. In this notation, disorder is defined as

$$\Delta = \frac{S}{S_{max}}, \tag{13}$$

where S is the information entropy of the system. So, entropy and disorder are decoupled in the Landsberg definition. Order is defined as,

$$\Omega = (1 - \Delta). \tag{14}$$

$\Omega = 1$ denotes a system that is perfectly ordered and predictable. SDL complexity is defined as,

$$\Gamma_{\alpha\beta} = \Delta^\alpha\Omega^\beta = \Delta^\alpha(1-\Delta)^\beta = (1-\Omega)^\alpha\Omega^\beta \tag{15}$$

It defines the complexity of disorder strength α and order strength β. The definition of the LMC measure is written as

$$C = S.D \tag{16}$$

S stands for the information content that is generated in the system and it is defined as $S = S_x + S_k$. The value D indicates the disequilibrium of the system.

$$D = D_x.D_k \tag{17}$$

we use the formula $C = S.D$ to numerically compute the LMC measure of complexity, and we use the formula $\Gamma_{\alpha\beta} = \Delta^\alpha\Omega^\beta$ to numerically calculate the SDL measure of complexity as a function of the lattice depth parameter V_0.

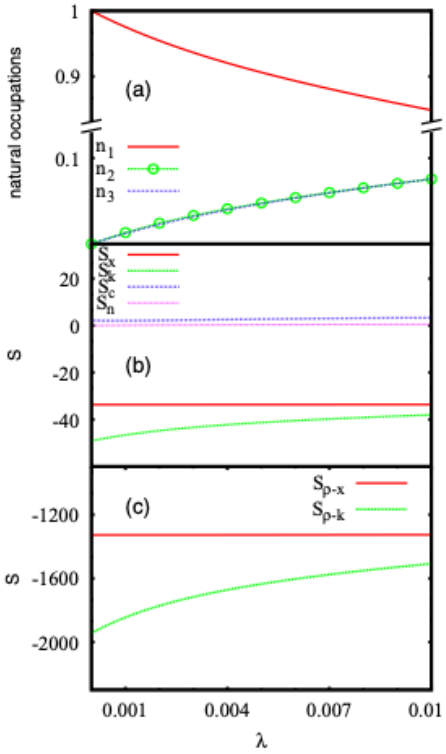

Figure 1: Occupation and entropy plot as a function of interaction strength for $\nu = 7$ and $N = 21$. (a) Natural occupation is plotted as a function of interaction strength. (b) Plot of one body Shannon information entropy in position space (S_x) and in momentum space (S_k), coefficient Shannon Information entropy (S_c) and orbital Shannon Information entropy (S_n). (c) Plot of two body Shannon information entropy in position space ($S_{\rho-x}$) and in momentum space ($S_{\rho-k}$).

4 Results

In this section, I will discuss the findings that I have obtained during my doctoral studies. In one of our works, we have solved the time independent Schrödinger equation for bosons trapped in one dimensional optical lattice potential and interacting via contact interparticle interaction ($W = \lambda\delta(x-x')$. It is already known that a few bosons with contact interparticle interactions in small optical lattices show a range of quantum phases. These quantum phases include superfluid, Mott-insulator, and fermionized Tonks gases. We have investigated all these phases through the measure of many-body Shannon information entropy, occupation in natural orbitals and Glauber's normalized correlation measurements. In another work, we have studied the time dynamics of interacting bosons followed by a quench from small repulsive interaction to large repulsive interaction. Firstly, bosons are loaded in a shallow optical lattice. When the interaction strength is suddenly increased while the lattice depth remains constant, the phase transition occurs. We use this system to study the quantum phase transition between a superfluid phase to a Mott-insulator state. The system's phase diagram describes the static features of the many-body state as a function of interaction strength. Our key measures for this work are Shannon information entropy, occupation in natural orbitals and fidelity decay. Our main goal was to describe relaxation processes in which different observables of this interacting quantum many-body system dynamically converge to equilibrium values over time.
In a separate work, we have quenched the optical trap keeping the interaction strength fixed and study the dynamics of the system. We have previously investigated the static and the time evolution of a bosonic system using variable contact interparticle interaction. In this work, we have chosen long range interaction having the form $W(x_i - x_j) = \frac{g_d}{|x_i - x_j|^3 + \alpha_0}$. Where g_d is the strength of the interaction. Nature of this interaction is discussed in Sec.4.3. Here, we set up the system in an asymmetric double well potential so that all bosons occupy the energetically favourable well and then we make the trap symmetric at $t = 0.0$. We have extracted four kind of dynamics, (i) Josephson oscillation, (ii) deformed Josephson oscillation, (iii) self trapping and finally (iv) equlibration. We characterize the above four phases by measuring population in each orbitals, fragmentation dynamics and two-body density measures. In a separate work, We would like to follow the path from the SF phase to the insulating phase by directly monitoring the change in order, disorder, and complexity. Our main focus is on investigating the transition from the SF phase to the MI phase via the non-monotonic dependency of SDL and LMC complexity on the lattice depth parameter. We successfully demonstrate that LMC complexity is a more comprehensive measure and may be utilised as a "figure of merit" to determine the time-scale with high precision. In order to solve the many-boson Schrodinger equation, we employ the multiconfigurational time-dependent Hartree method for bosons (MCTDHB) for all our studies. The findings are detailed in the following sections.

4.1 Study of different phases in optical lattice

Experiments in one-dimensional optical lattices with strongly interacting bosons have been demonstrated to be more troublesome than in three-dimensional ones as quantum fluctuation plays an important role in reduced dimension [Hal81, HGM+09, KWW04b]. A bose gas in a moderately deep optical lattice exhibits the superfluid phase for weak interparticle interactions. The superfluid state can be described as a state in which all particles are delocalized across all lattice sites. When the repulsive interaction or the depth of the optical lattice is comparatively large, each site is filled with the same number of bosons, and there is no longer any coherence between the sites — the many-body state enters the phase called Mott insulator phase [JBC+98, GME+02b, HHM+10]. When a single lattice site shares more than one bosons, due to their repulsion within the lattice site, the system shows a new phase called fermionized phase. Bose-Hubbard model is often used to illustrate the zero-temperature transition from superfluid to Mott insulator state. But its regime of validity is limited to situation in which site-localized Wannier states perform as an appropriate basis set. Thus in the regime of strongly interacting bosons, Bose-Hubbard model fail. For this research work, we are trying to understand how the transition from superfluids through Mott insulator to fermionized phase can be explained in terms of many-body information entropy and Glauber's normalized correlation functions. For this work, we have consider three different scenario for different number of particles loaded in three well optical lattice having the form $V(x) = V_0 sin^2(kx)$, where $k = \frac{\pi}{d}$. d is the periodicity and V_0 is the depth of the optical lattice. For the entire calculation, we fixed the lattice depth at $V_0 = 12.0$. In our one dimensional case, we choose the grid point from $x_{min} = -\frac{3\pi}{2}$ to $x_{max} = \frac{3\pi}{2}$ so that we consider three well for the entire calculation. The Hamiltonian for N number of interacting bosons is

$$H = \sum_{i=1}^{N} \left(-\frac{1}{2}\frac{\partial^2}{\partial x_i^2} + V(x_i) \right) + \lambda \sum_{i<j}^{N} \delta(x_i - x_j). \tag{18}$$

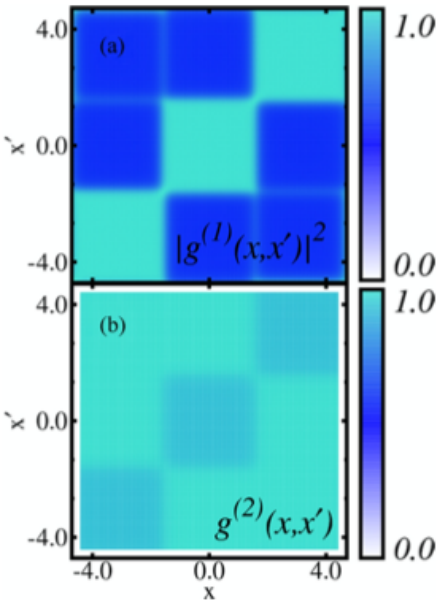

Figure 2: (a) First-order normalized correlation function $|g^{(1)}(x',x)|^2$ and (b) second-order normalized correlation function $|g^{(2)}(x',x)|$ for the superfluid phase. The interaction strength is $\lambda = 0.01$, number of particle $N = 21$ and $\nu = 7$

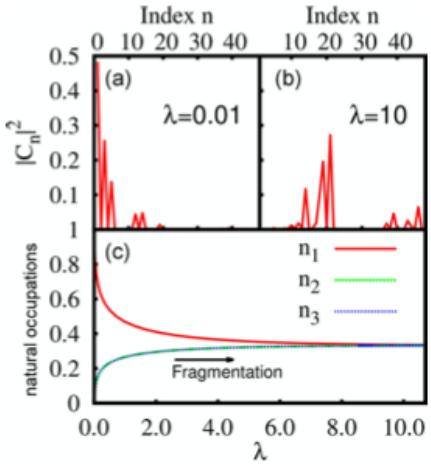

Figure 3: The distribution of the magnitude of the coefficients $|C_n|^2$ as a function of the index n for $\lambda = 0.01$ in (a) which is a superfluid state and for interaction strength $\lambda = 10.0$ in (b) which is a Mott insulator state. (c) Natural occupation of the first three orbitals as a function of interaction strength. At $\lambda \simeq 6.0$, the state is three fold fragmented ($n_1 \simeq n_2 \simeq n_3 \simeq \frac{1}{3}$).

λ is the strength of the contact interparticle interaction and can be tuned experimentally by manipulating the strength of the transverse confinement. We introduce a quantity, filling factor (ν), which is the ratio of the number of atoms N to the number of lattice sites W: $\nu = \frac{N}{W}$. In this work, we focus on the cases of commensurate filling factor $\nu = 1$,2 and 7. This section will first discuss the superfluid state with $\nu = 7$ for weak interaction strength. We took $N = 21$ particle in three well optical lattice. In Fig 1(a), we plot the natural occupation in the orbitals as a function of interaction strength. Superfluid phase occurs at weak interaction strength, so we keep our interaction from zero to 0.01. From the natural occupation, it is clear that major contribution comes from the first orbital and contribution from second and third orbitals are below 10%. So, our $\nu = 7$ case can be considered as a condensate at this interaction strength according to Panos and Onsagar criteria [PO56]. Thus this state can be represented as a single-orbital mean-field state $|N, 0, 0\rangle$. This is to be noted that $M = 3$ orbital is sufficient for converged result. Adding another orbital does not change the many body state quantitatively.

We plot the one-body Shannon information entropy for density and momentum space as a function of interaction strength λ in Fig 1(b). As λ increases, density in coordinate space increases and same in momentum space decreases. As a result, S_x decreases and S_k increases. We have also present coefficient Shannon information entropy (S_c) and information Shannon information entropy (S_n) in Fig 1(b). As obvious from the definition, S_c and S_n are very close to zero, because only one single particle state is contributing in this calculation. Macroscopically occupied single-particle state like the Gross-Pitaevskii mean-field equation can provide a suitable explanation of this state.

In Fig 1(c), we plot the two-body Shannon information entropy for coordinate and momentum space as a function of interaction strength λ. The two-body Shannon information entropy behaves similarly to the one-body entropy measures. However, $S_{\rho x}$ increases in a higher rate compare to that in S_x and, similarly, the rate of decrease of $S_{\rho k}$ is faster than that in S_k. In fact the two body density matrix — from where the two body Shannon information entropy is derived — can be written as the product of one-body densities for a superfluid phase.

In Fig 2(a), we plot the normalized first order correlation function $|g^{(1)}(x',x)|^2$ for $\lambda = 0.01$. We can see in the (x,x') region where the density is high, $|g^{(1)}|^2$ have the value 1. This is led to believe that coherence inside indivisual lattice site as well as between different lattice sites is preserved. In Fig 2(b), we plot the normalized second order correlation function $|g^{(2)}(x',x)|$ for $\lambda = 0.01$. $|g^{(2)}(x',x)| \simeq 1$ means that the coherence between the different wells is being perfectly maintained. There is a not so prominent structure trying to build around $x = x'$: implies that antibunching effect starts to develop due to repulsive interaction within the same sites.

Now, we will examine the many-body physics of the Mott insulating phase using correlation functions, coherence, and Shannon's information entropies. To produce the conventional Mott insulator phase in strong interaction regime,

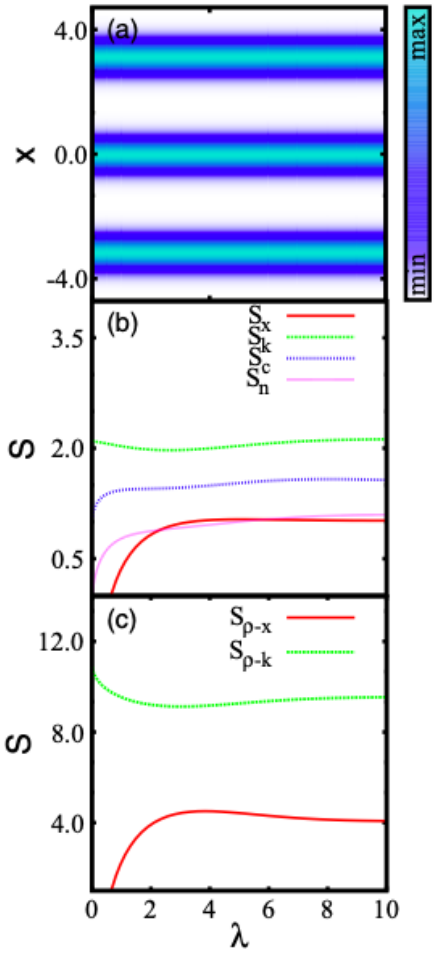

Figure 4: One-body density and entropies in the superfluid to Mott-insulator transition as a function of the interaction strength for three bosons in three well optical lattice. (a) One-body density is plotted as a function of interaction strength. (b) Plot of one body Shannon information entropy in position space (S_x) and in momentum space (S_k), coefficient Shannon Information entropy (S_c) and orbital Shannon Information entropy (S_n). (c) Plot of two body Shannon information entropy in position space ($S_{\rho-x}$) and in momentum space ($S_{\rho-k}$).

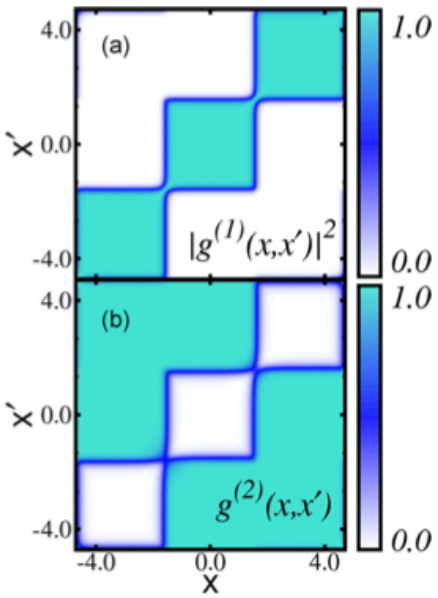

Figure 5: (a) First-order normalized correlation function $|g^{(1)}(x', x)|^2$ and (b) second-order normalized correlation function $|g^{(2)}(x', x)|$ for the Mott-insulator phase. The interaction strength is $\lambda = 0.01$, number of particle $N = 3$ and $\nu = 1$

we consider $N = 3$ bosons in three wells i.e., one atom per site and $\nu = 1$. In Fig 3(a) and Fig 3(b), we plot the expansion coefficient $|C_n|^2$ for $\lambda = 0.01$ and $\lambda = 10.0$ respectively. $\lambda = 0.01$ corresponds to superfluid state and $\lambda = 10.0$ puts the system in Mott insulator state. The total number of configuration which is available for the system is $N_{conf} = \begin{pmatrix} N+M-1 \\ N \end{pmatrix}$. In our calculation, we take $M = 6$ for convergence. So the possible configuration is 56. For superfluid phase, the coefficients expands only in a small portion of the total allotted space. We refer such state as localized state. Whereas for Mott insulator state, as the interaction is strong enough, the coefficients expand over all possible space. We refer such state as delocalized state.

In Fig 3(c), the occupation of the first, second, and third natural orbitals as a function of interaction strength is plotted. With increase in interaction strength, the occupation of the first natural orbital drops gradually while the occupations of the second and third natural orbitals grow considerably. At sufficient interaction strength, contribution from the first three orbitals marge to a equal value. Contribution from all three orbitals are 33.33% each. The contribution from the other three orbitals are of the order of 10^{-7}, which is negligibly small. We called this state is three fold fragmented state. This apparently indicates that the loss of coherence of distinct sites. Thus the path from single orbital contribution to three fold fragmentation with increase in interaction strength is basically superfluid to Mott-insulator transition. It is also called the interaction strength driven condensate to fragmented state transition.

In Fig 4(a), we plot the one-body density as a function of interaction strength. As $\nu = 1$, density is same throughout the interaction region, each sites are occupied by one boson. The superfluid to Mott insulator transition cannot be described by density alone. For further study, we have examined the one-body Shannon information entropy for density and momentum space, coefficient Shannon information entropy and orbital Shannon information entropy as a function of interaction strength and plotted in Fig 4(b). When interaction strength is small S_x and S_k has minimum value and saturates at larger interaction strength. It is important to notice that coefficient Shannon information entropy (S_c) and orbital Shannon information entropy (S_n) have value nearly zero when the interaction strength is very small. It implies that only one orbital is contributing significantly. This phase is purely a superfluid state. As λ increases, S_c and S_n rises. When the state reaches the three fold fragmented Mott insulator state, S_c and S_n saturates to a finite value. We will now investigate this saturation values of entropies with the prediction from Gaussian orthogonal ensemble (GOE). Our calculation has an excellent match with the result from GOE values. In Fig 4(c), we present our result for two-body Shannon information entropy for density and momentum space. These results also shows the same kind of behaviour.

Figure 5 depicts an analysis of the first- and second-order coherence in the fragmented Mott insulator for $\lambda = 10.0$. The diagonal of the first-order correlation function identifies three entirely unique coherent zones where which implies the coherence within the same well is maintained whereas it is lost across different wells. $|g^{(1)}(x', x)|^2 \simeq 1$.

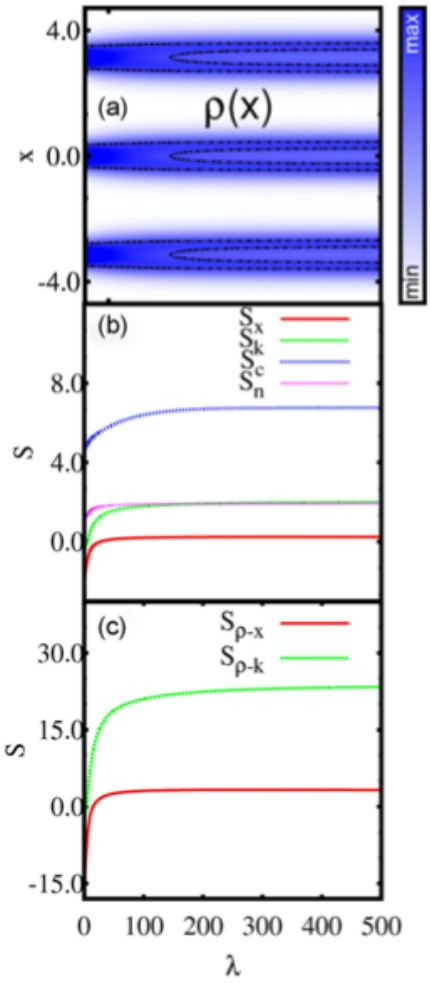

Figure 6: One-body density and entropies in the superfluid to Mott-insulator to fermionization transition as a function of the interaction strength for six bosons trapped in three well optical lattice. (a) One-body density is plotted as a function of interaction strength. (b) Plot of one body Shannon information entropy in position space (S_x) and in momentum space (S_k), coefficient Shannon Information entropy (S_c) and orbital Shannon Information entropy (S_n). (c) Plot of two body Shannon information entropy in position space ($S_{\rho-x}$) and in momentum space ($S_{\rho-k}$).

In Fig 5(b), we plot the second-order coherence. $g^{(2)} \simeq 0$ along the diagonal and $g^{(2)} \simeq 1$ along the off-diagonal. $g^{(2)} \simeq 0$ along the diagonal refers as the correlation hole which signifies that chances of finding two particle at the same well is zero. $g^{(2)} \simeq 1$ at off-diagonal implies that probability of finding any two bosons in two different wells are always one.

We will now characterise the phases of a system that shares two bosons at each site by utilising the density, normalised correlation functions, and Shannon information entropy measurements. In lattices with a commensurate filling factor of more than one, which means that there is more than one boson per site, the strength of the interactions between the particles can cause two type of phase transitions. One that we have already discussed for $\nu = 1$ is the superfluid to Mott insulator transition. It happens when the interaction strength is moderate. The other one is the Mott insulator to fermionization transition which happens at large repulsive interaction limit. One can observe this transition only when $\nu > 1$. Our main motivation here is to study the Mott insulator to fermionization transition. In order to study this transition, an optical lattice with a filling factor of two can be used as the generic system. As discussed earlier, superfluid to Mott insulator transition happens around $\lambda \simeq 10$. Now if we increase λ further, Mott insulator to fermionization transition happens. We increase λ sufficiently high ($\lambda \geq 200$) and plot the one-body density in Fig 6(a). In this instance, the bosonic density mimics the fermionic density in which Pauli exclusion prohibits the spatial overlap of particles. Two bosons sharing each well repeal each other due to strong repulsion. This reflects in the density structure— splitting of density within the well.

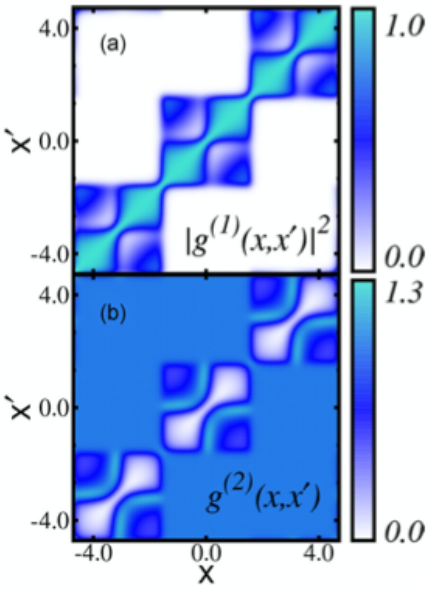

Figure 7: a) First-order normalized correlation function $|g^{(1)}(x', x)|^2$ and (b) second-order normalized correlation function $|g^{(2)}(x', x)|$ for the feermionized phase. The interaction strength is $\lambda = 200$, number of particle $N = 6$ and $\nu = 2$

The corresponding Shannon information entropy both for one-body and two-body are plotted in Fig 6(b) and in Fig 6(c). It is important to note that fermionization takes place at much higher interaction strength($\lambda \simeq 200$). So all the entropy measures increases up to that value and then tries to saturate. At considerably higher interaction strengths, saturation is reached.

In Fig 7, we plot the first- and second-order coherence in the fermionized limit for $\lambda = 200$. Both $|g^{(1)}|^2$ and $g^{(2)}$ exhibit same nature as of Mott insulator state: $g^{(1)2}$ has only diagonal terms and $g^{(2)}$ has off diagonal terms. The new thing of fermionization is that two particle sharing one well and due to strong inter-particle interaction, the two patches in each well is prominent in both $|g^{(1)}|^2$ and $g^{(2)}$.

4.2 Dynamical study of interacting bosons in optical lattice.

In the last decade, the non-equilibrium dynamical features and statistical relaxation, in which multiple observables of an isolated and interacting quantum many-body system dynamically converge to equilibrium values, have attracted a lot of attention. Experiment on cold atoms in optical lattice investigations have had a huge impact on this subject. Theoretically, the thermalization of an isolated quantum system is a well-established fact and the system thermalization happens when the measuring quantities have the same values as of their long time average values given by Gibbs ensemble. The main focus of this study is to investigate how the system evolves after a sudden quench from small interaction strength to large interaction strength. It is known that bosons loaded in optical lattice show different phases like superfluid, Mott-insulator, fermionized etc. Our study also investigate how system changes from one phase to another phase during this time evolution. We also give a brief idea how the system thermalizes. The statistical relaxation of various dynamical variables to some sort of equilibrium is a requirement for thermalization. The Shannon information entropy is one of these fundamental dynamical variables that follows this relaxation. Another quantity we introduce here is the survival probability or simply the quantum fidelity. It is defined as $F(t) = |\langle\psi(t = 0)|\psi(t)\rangle|^2$ and thermalization in a optical lattice can be predicted from the power-law behaviour of $F(t)$.

Here we present the relaxation dynamics of $N = 3$ number of interacting bosons in a triple-well lattice. We initially setup the system in the superfluid phase and trigger dynamics in the system through a quench to a different interaction strength. The strength of the quenching interaction has a range from a weak to a high one in this study. With the help of the measured variable — occupations of the different natural orbitals $n_i(t)$, the quantum fidelity $F(t)$ and the many-body information entropy $S^{info}(t)$, We establish a connection between the fragmented many-body state, the collapse of quantum fidelity, and the equilibrium saturation of the many-body information entropy.

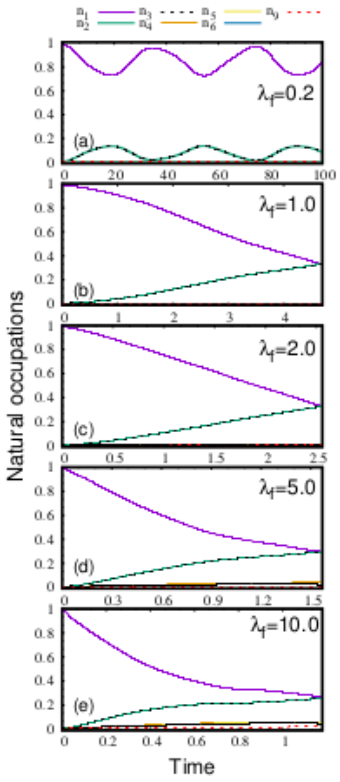

Figure 8: Propagation of the natural occupations $n_i(t)$ for different interaction quenches. (a) $\lambda_f = 0.2$, (b) $\lambda_f = 1.0$, (c) $\lambda_f = 2.0$, (d) $\lambda_f = 5.0$, (e) $\lambda_f = 10.0$. For stronger interactions, it takes less time to encounter threefold fragmentation.

Initially we prepare the system of $N = 3$ interacting bosons in three well optical lattice and solve the many-body Schrödinger equation 18. The depth of the optical lattice is chosen as $V_0 = 3.0$. We tweak the interaction strength and analyze the dynamics followed by the quench while keeping the lattice depth constant. The system will transit from superfluid to Mott-insulator state when we increase the interaction strength (discussed in sec. 4.1). For this case, the transition interaction strength (λ_c) for which the phase transition take place is $\lambda_c \simeq 0.4$. The ground state is prepared at $\lambda_i = 0.05$: which is a superfluid state. Then we quench the Hamiltonian to λ_f so that $\lambda_f > \lambda_i$. In the ground state, the bosons are delocalized over the entire lattice and one single orbital is sufficient to describe this state. When we quench the system to interaction strength λ_f, we are basically pumping the energy of the system. The excitation energy of the system is given by $E_{ex} = E(\lambda_f) - E(\lambda_i)$ and presented in Table. 1.
First we consider the time evolution of the system through natural occupation in time dependent orbitals. We quenched the system for five different λ_f and the results are presented in Fig 8. Initially when the system is in the ground state, only the first natural orbital is fully occupied, i.e., $n_1 \simeq 1$ and $n_i \simeq 0$ for $i > 1$. It is also verified from the natural occupation that the ground state is a superfluid state. For the static case (not shown here), superfluid to Mott-insulator transition happens at $\lambda_c = 0.4$. But the dynamics are different from that of static case. Firstly, we quench the system to $\lambda_f = 0.2$ which is less than λ_c. As plotted in Fig 8(a), population in second and third orbitals are oscillating with time having the maximum value ($\simeq 0.14$). We called this state as fragmented but not three

Table 1: Value of different interaction quench parameter, the corresponding excitation energy and the character is time when the system reaches first time to the Mott insulator state.

λ_f	E_{ex}	t_c
0.2	0.061	N.A.
1.0	0.263	4.70
2.0	0.667	2.56
5.0	1.878	1.57
10.0	3.898	1.18

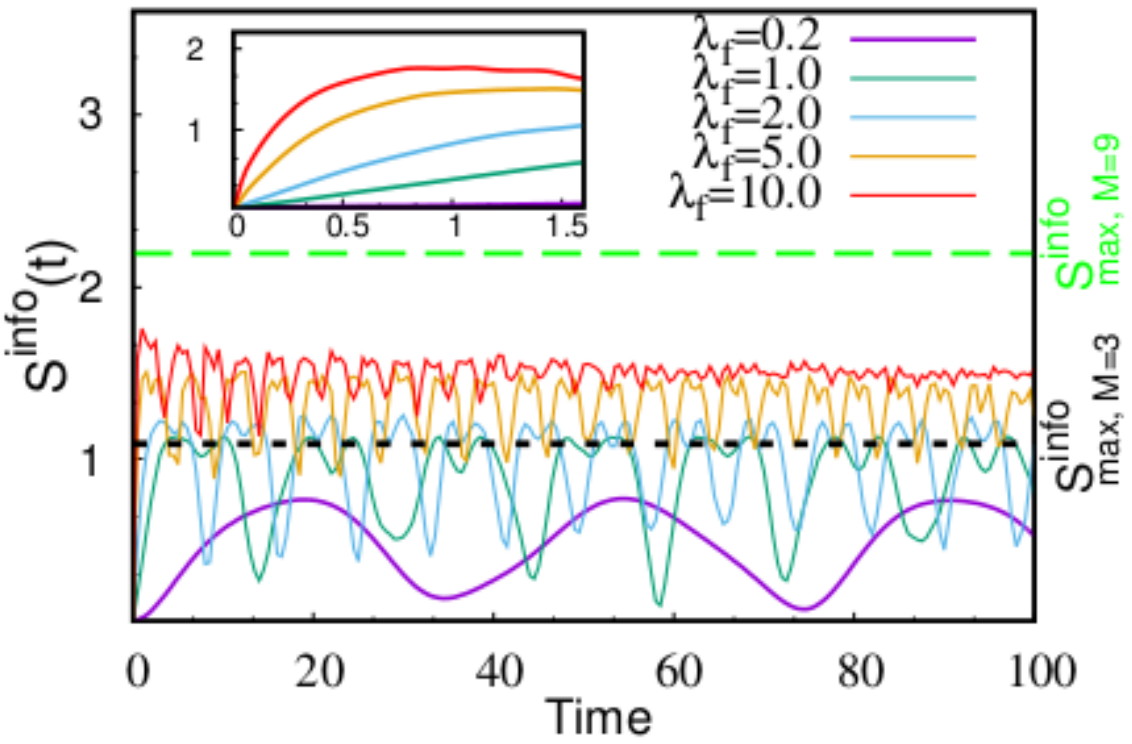

Figure 9: Propagation of the natural occupations $n_i(t)$ for different interaction quenches. (a) $\lambda_f = 0.2$, (b) $\lambda_f = 1.0$, (c) $\lambda_f = 2.0$, (d) $\lambda_f = 5.0$, (e) $\lambda_f = 10.0$. For stronger interactions, it takes less time to encounter threefold fragmentation.

fold fragmented Mott insulator state. If the quench is carried out in such a way that $\lambda_f > \lambda_c$, then the threefold fragmentation will take place at some time and that repeats itself multiple times, almost on a periodic basis (not shown here). We define a characteristic time t_c when the first threefold fragmentation occurs. We can easily find t_c from Fig 8 and it is presented in Table. 1. At t_c, the system is threefold fragmented, i.e., $n_1 \simeq n_2 \simeq n_3 \simeq 1/3$. From Table. 1, one can easily found that characteris tic time t_c decreases as λ_f increases. It is probably because of the increased amount of energy that the quench put into the system.

Now we will discuss the time evolution of occupational Shannon information entropy ($S^{info}(t)$). $S^{info}(t)$ is plotted in Fig 9 as a function of time for different λ_f. For small interaction quench ($\lambda_f = 0.2$), $S^{info}(t)$ exhibits oscillation, which mimic the collapse revival dynamics. For quenches $\lambda_f > \lambda_c$, entropy shows a rapid increase upto t_c (shown in the inset of Fig 9). Thus when the system transit from superfluid to Mott insulator state, entropy increases rapidly and attains a maxima when the system reaches to Mott insulator state. This maximum value attains ta $t = t_c$. At long tim dynamics, entropy oscillates for quenches to $\lambda_f = 1$ and 2. These oscillations point to the fact that the system passes through a periodic dynamical shift between a threefold fragmented MI state where the entropy is at its highest and a condensed state where the entropy is at its lowest on a regular basis. In the case of quenches with a stronger interaction strength, $\lambda_f \geq 5$, the occupation entropy reaches maximal values that are greater than the one that is expected for a threefold fragmentation of the system ($S^{info}(t) > ln(M) = ln(3) = 1.099$). The reason is that more than three orbitals are contributing in the time evolution. This can be seen in Fig 8(d) and Fig 8(e), where the contribution from the lower orbitals are also significant. For $\lambda_f = 10.0$, entropy oscillation decays over time and finally saturates to a value. So, we can say that when the quantum quenches to a high interaction strength, the entropy settles down to a certain value.

The role of the many-body eigenstates in the dynamics by looking at how the fidelity has changed over time is another importent tool to study. The time evolution of quantum fidelity is presented in Fig 10. For small interaction strength ($\lambda_f = 0.2 < \lambda_c$), fidelity remain close to unity (Fig 10(a)). In this scenario, the system is only slightly fragmented, and as a result, the time-evolved wave function strongly overlaps with the initial one. When quenching to higher levels of interaction strength, such as $\lambda_f = 1$ and 2, the fidelity shows a dips first at the characteristic time t_c and then repeats the same after a time interval. When there is a very small overlap

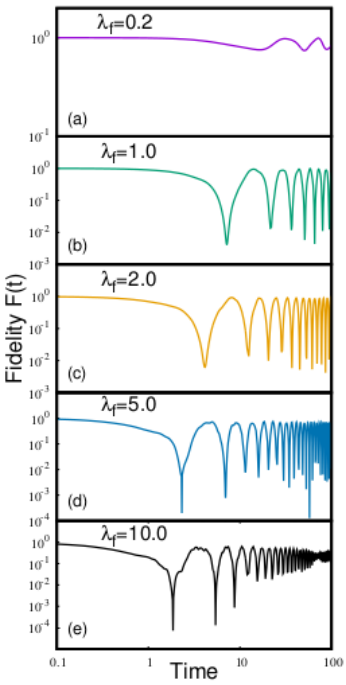

Figure 10: Propagation of the natural occupations $n_i(t)$ for different interaction quenches. (a) $\lambda_f = 0.2$, (b) $\lambda_f = 1.0$, (c) $\lambda_f = 2.0$, (d) $\lambda_f = 5.0$, (e) $\lambda_f = 10.0$. For stronger interactions, it takes less time to encounter threefold fragmentation.

between the current state and the initial state, the fidelity drops significantly. In our perception, the dips are an indicator of the dynamical transition to the MI state. At very high interaction strength ($\lambda_f \geq 5$), dips become "spikes" at $t = t_c$, a non-analytical point in the fidelity function that we term the collapse point. At this point, once the MI state has been reached, there is a significant reduction in the amount of overlap with the initial state. This non-analytical behaviour is similar to the non-analyticity of the Loschmidt echo rate function in dynamical quantum phase transitions. Thus, we demonstrated the characteristics of relaxation for an isolated quantum system and its relationship to a dynamical quantum phase transition marked by a collapse point in quantum fidelity.

4.3 Quantum dynamics in double well potential

Macroscopic coherent effects and many-body features can be studied using the tunnelling quantum dynamics of ultracold atoms in double well potentials [SFGS97]. Experimentally, it is possible to make direct observations of tunnelling as well as nonlinear self-trapping for ultracold bosons [CCP04, AGF+05, AAG+05, SKH+06] and fermions [NSR18, BSA+18, LSB+20, KPP+20], and this is true for both double- and multi-well potentials. In this section, we investigate the dynamics of dipolar bosons in one-dimensional double-wells. By increasing the strength of the contact interaction and analysing the one-body observables and two-body correlation dynamics, we study tunnelling oscillations, self-trapping, and a regime in where the system exhibit equilibration behaviour. The interatomic correlation and inter-well coherence play an important role in two-body correlation dynamics because of the non-local nature of repulsion. We also look at the connection between the correlation dynamics and the way natural orbitals in the one-body density matrix are filled. The mean-field model and the quantum two-mode model were used to study the properties of dipolar bosons in a double well potential. The many-body dynamics of bosons with non-local interactions have been studied recently for finite range interaction. In our work, we investigate the effect of long-range interaction in the double well tunneling dynamics. The dipolar interaction is modeled as

$$W(r) = \frac{g_d}{r^3 - \alpha_0} \tag{19}$$

where $r = |x_i - x_j|$ is the distance between two particle. The dipolar interaction strength is g_d and α_0 is the cut-off parameter to avoid the divergence at $xi_{=}x_j$. g_d can be tuned experimentally. Throughout this section, we keep $g_d > 0$ such that we consider repulsive dipolar interacting bosons. We solve the many-body Schrödinger equation

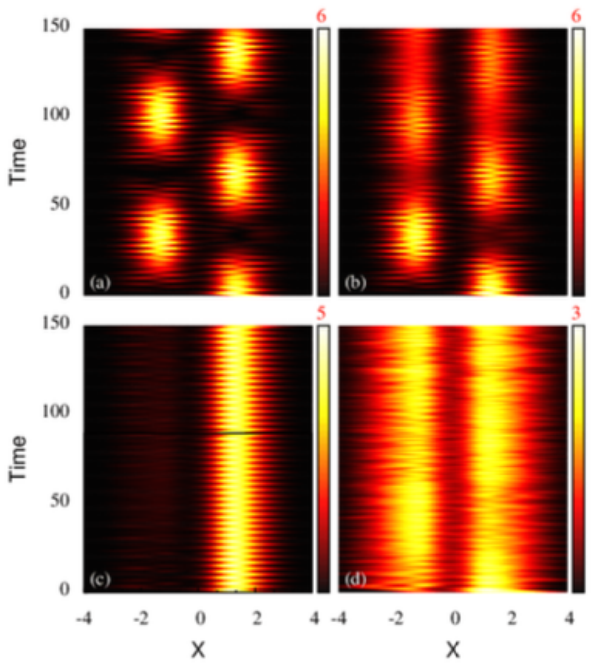

Figure 11: Tunneling dynamics of $N = 6$ interacting dipolar bosons in a double-well potential with varying interaction strengths g_d. The population of the left and right wells is shown as a function of time. (a) $g_d = 0.0$ exhibits Rabi oscillations. (b) $g_d = 0.002$ showcase deformed Rabi oscillations. (c) $g_d = 0.02$ shows self trapping of all bosons in the right well. (d) $g_d = 0.2$ exhibits equlabration.

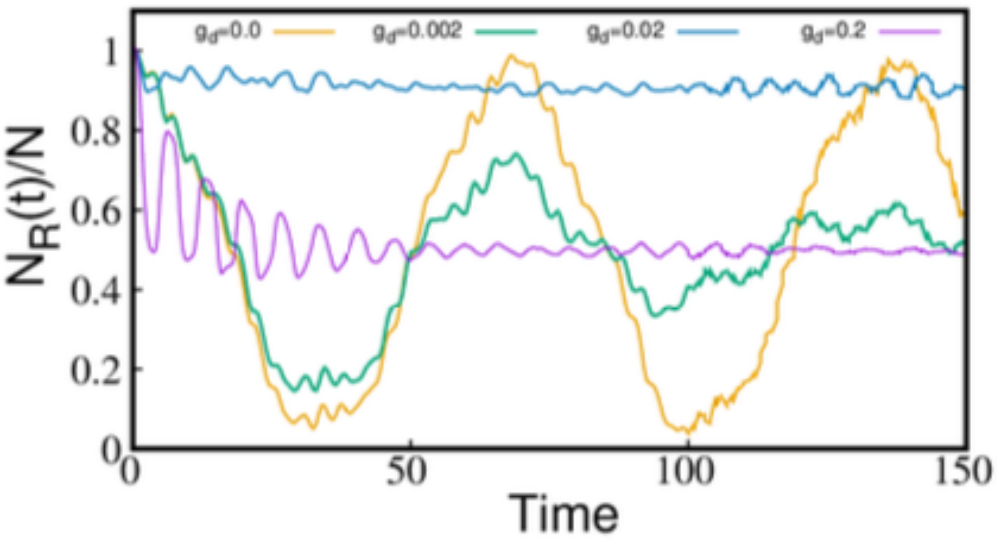

Figure 12: The variation of the relative population in the right-hand well ($\frac{N_R(t)}{N}$) as a function of time for different interaction strength.

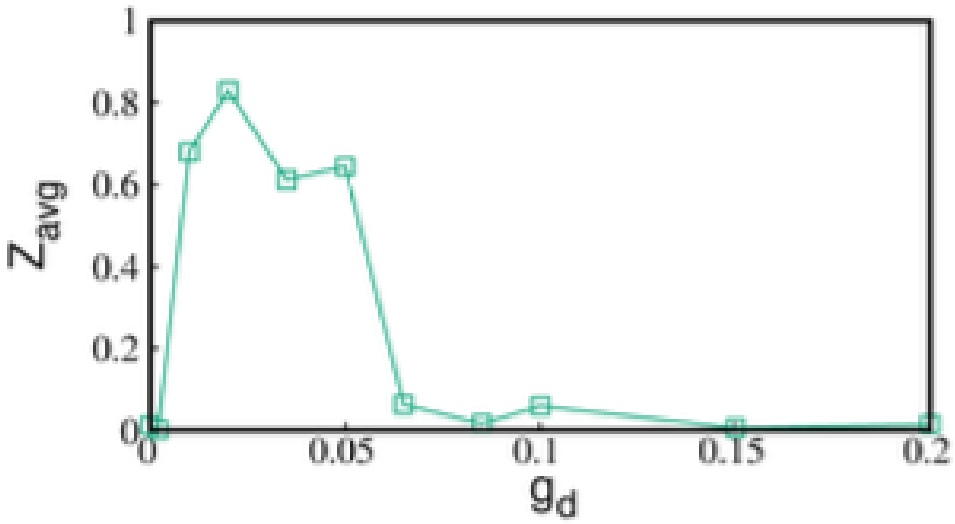

Figure 13: Average population imbalance as a function of interaction intensity g_d. The peak point implies maxumim self trapping.

given by,

$$\hat{H}(x_1, x_2, \ldots, x_N) = \sum_{i=1}^{N} \hat{h}(x_i) + \sum_{i<j=1} \hat{W}(x_i - x_j) \tag{20}$$

where $\hat{h}(x) = \hat{T}(x) + \hat{V}(x)$ is the one-body term of the Hamiltonian. $V(x)$ is the asymmetric double well potential considered as,

$$V(x) = \frac{1}{2}x^2 + V_0 \frac{e^{-\frac{x^2}{\sigma^2}}}{\sqrt{\pi}\sigma} - dx, \tag{21}$$

d denotes the asymmetric parameter. The double well becomes symmetric when $d = 0$. For $N = 6$ dipolar bosons, we solve the time-dependent Schrödinger equation. The one-body density, the population in the right well, the population imbalance, and the two-body density for various g_d values are used to analyze the tunnelling dynamics.To make the right well more energetically favourable, d is initially kept quite large. So all bosons are in the right well initially. To make the double well asymmetric, we choose $d \neq 0$. V_0 is kept at 8.0 and $\sigma = 0.7$. To achieve convergent findings throughout our work, we do the computation with $M = 10$ orbitals. Comparing the quantities computed with $M = 10$ and $M = 12$ orbitals, we found insignificant quantitative differences. Convergence is also secured because to the near-zero occupied in the last orbital. Here we take four interaction regime: (1) $g_d = 0.0$ is the non-interacting case, (2) $g_d = 0.002$ is the weak interaction regime, (3) $g_d = 0.02$ is moderate interaction regime and (4) $g_d = 0.2$ is the strong interaction regime. Firstly we discuss the tunneling dynamics through the measure of one-body density. The detail method to calculate one-body density is thoroughly discussed in sec 3. We calculate $\rho(x, t)$ upto time $t = 150$ for all four choices of g_d and presented in Fig 11. In non-interacting limit ($g_d = 0.0$), the atoms are simply exhibiting Rabi oscillation between the two wells. In the low interaction limit ($g_d = 0.002$), we observe tunneling dynamics but because of the repulsive tail of non-local interaction, the frequency and amplitude of oscillations in tunnelling has been significantly affected. When g_d is set to 0.02, the tunnelling dynamics exhibit self-tapping: for long periods of time, the right well's population has remained nearly constant. We find the same self-trapping behaviour when considering contact interaction (which is not shown here), but for significantly higher interaction strength. The long-range repulsive tail of the dipole interaction appears to be the cause of the self-trapping at a relatively weak interaction. But quantum fluctuations prevent bosons from remaining in the self-trapped state for long periods of time, no matter how many particles they have. For strong dipolar interaction ($g_d = 0.2$), Particles settle in equal numbers in both wells, resulting in an equilibration dynamics.

Further, we calculate the population in the right well utilising the formula

$$N_R(t) = \int_0^\infty \rho(x, t)dx \tag{22}$$

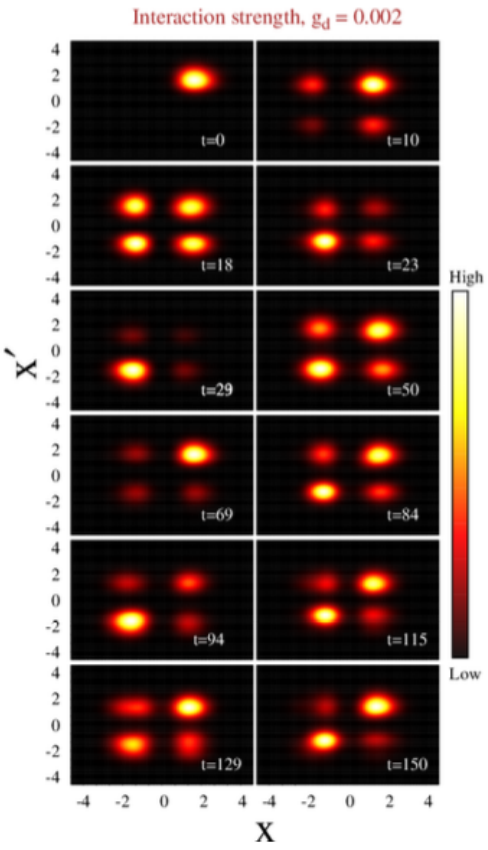

Figure 14: Time evolution of two body density for dipolar interaction strength $g_d = 0.002$. Initially all particles Seattle in right well. Particles began tunnelling with the change in time. Furthermore, this image confirms the deformed Rabi oscilation for $g_d = 0.002$

and $\frac{N_R(t)}{N}$ is presented in Fig 12 as a function of time. Non-interacting bosons shows Rabi's oscillation. For $g_d = 0.002$, upto time $t \simeq 80$, system tries to oscillates with Rabi's frequency but in long time dynamics, partial equilibrium is seen, with $N_R(t)/N$ trying to reach its saturation point at 0.5. When we increase the interaction strength ten times, i.e., $g_d = 0.02$, we observe $N_R(t)/N$ close to unity. It indicates all particles are sattle in the right well, makes this state self trapped. According to our best estimations based on data from the right well's population, this state is close to 90% self trapped. For $g_d = 0.2$, The system exhibits a unique type of single-scale dynamics, namely equilibration, wher $N_L = N_R = 3$. In addition, we calculate the population imbalance as

$$Z(t) = \frac{N_R(t) - N_L(t)}{N} \qquad and \qquad Z_{avg} = \frac{1}{t}\int_0^t Z(t')dt' \tag{23}$$

In Fig 13, we have plotted Z_{avg} as a function of time. It exhibits crossover between the four types of dynamics described above. Rabi oscillation for non-interacting limit and equilibration dynamics in the case of strong interaction have Z_{avg} equal to zero. The maximum amount of population imbalance happens at a certain interaction strength g_d^c, which is equivalent to self-trapping. Therefore, a qualitative estimate of the interaction regime for self-trapping can be obtained by looking at the breadth of the curve.

Next, we study how the effect of two-body correlation comes into play in the dynamics by studying the two-body density over time for increasing interaction strength, g_d. The impact of two-body correlation is assessed by the competition between the non-local interaction and the inter-well coherence when interaction is turned on. As a result, the dynamics of the two-body correlation are considered to be difficult. Non-interacting bosons tunnel independently and aren't presented in this synopsis. We starts with $g_d = 0.002$. Two-body density snapshots taken at various points in time are depicted graphically in Fig 14. At this weak interaction, bosons initially accumulate in the right well. However, during tunnelling, we observe competition between the correlation due to the inter-well coherence and non-local interaction. Due to repulsive long range interaction, bosons start to tunnel. During the course of tunneling, at time $t = 18$, we observe four equal bright spot two along diagonal ($x = x'$) and two

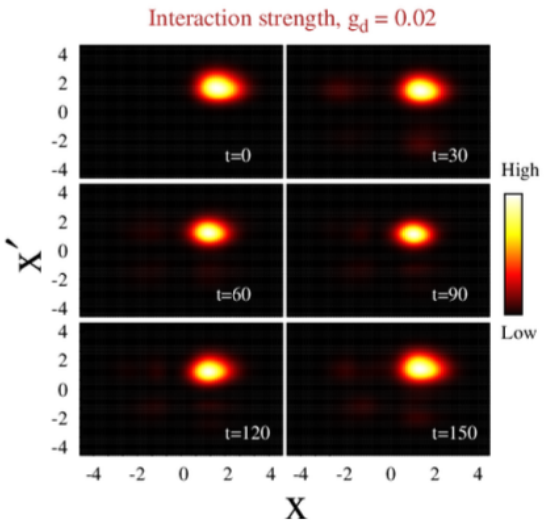

Figure 15: Time evolution of two body density for dipolar interaction strength $g_d = 0.02$. Initially all particles Seattle in right well. During the course of time, bosons remain self-trapped in the right well.

along off-diagonal ($x = x'$) emphasizing the situation that inter-well coherence is preserved Thus, interatomic and inter-well correlations are sustained on the same scale. At this time, both well are sharing equal number of bosons ($N_L \simeq N_R \simeq 3$). Next, at $t = 29$, we detect the formation of a highly coherent cluster in the left well, indicating the loss of inter-well coherence and the dominance of interatomic correlation. As time progresses, we see an increasingly complicated conflict between interatomic correlations in either well and inter-well coherence, which leads in the Rabi-like oscillations depicted in Fig 12. Only two bright spots are seen along the diagonal at longer times ($t = 150$), which again corresponds to an equal population in two wells. But if we compare this equal population with that in time $t = 18$, we can draw the conclusion that by eliminating inter-well coherence, an equal population is achieved. In Fig 15, we plot the two-body density for interaction strength $g_d = 0.02$. As can be seen in the figure, the originally coherent cluster that formed in the right well has remained constant throughout time, a phenomenon known as self-trapping. The key role is played by the correlation between the atoms. A few faded spots appear along off-diagonal, indicating that complete self-trapping has not been achieved. To be consistent with Fig 12, which shows that around 90% of the self-trapping occurs when $g_d = 0.02$, it agrees well with this. In Fig 16, we plot the two-body density for stronger interaction strength $g_d = 0.2$. Repulsion tails have a substantial impact even at $t = 0$: the many-body state is incoherent and scattered compared which is missing in smaller interaction strength (Figs 14 and Fig 15). At $t = 10$, four bright patches appear, indicating that the populations in the two wells are equal. This equal population during the course of time has also achieved in Fig 14 ($t = 18$). Now, if we compare the two state, we can come to the conclusion that for stronger interaction, the bright spots have spread out, which means that three bosons in a well are feeling the effect of repelling each other. So, atoms in each well are incoherent. At longer time, if we compare the extreme two cases ($g_d = 0.2$ and $g_d = 0.002$), time $t = 150$ of Fig 14, we see almost the same number of bosons in both wells, but there is no coherence between them. Whereas, the same time of Fig 16 exhibit equilibration is preserved along with inter-well coherence. As a result, we have arrived at the conclusion that the dynamics that are observed for various combinations of interaction strength are fundamentally driven by the interplay that occurs between the inter-atomic correlation and the inter-well coherence.

4.4 Complexity in optical lattice

Various information theoretic measures have been put forward for consideration in many different scientific fields. It has been demonstrated that the information theoretical measures are the conceptually superior method for the investigation of structures present in a wide variety of system types [Hua13, AA08, TSMRD16, Ast19]. Within this framework, the idea of complexity has attracted a lot of attention due to its relevance [CMP05, AC00, SLR05]. The complexity measure is used to characterise how a physical or biological system would organise itself in response to a change in the external factors. The literature contains a number of different definitions of complexity [PCMK07, CGLR02, Sen11, LR05]; however, the standard definition of complexity, sometimes known as SDL complexity, was presented by Shiner, Davison, and Landsberg [SDL99]. This definition use the notation $\Gamma_{\alpha,\beta}$. The other statistical measure of complexity, given by the abbreviation C, is referred to as the LMC measure and

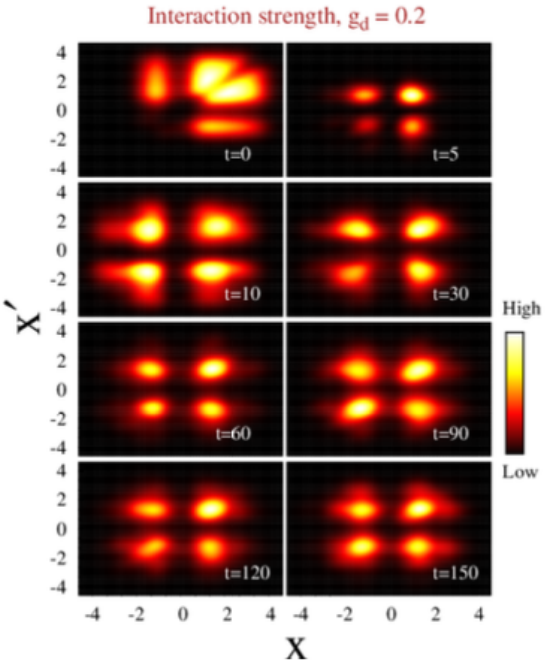

Figure 16: Time evolution of two body density for dipolar interaction strength $g_d = 0.2$. Initially all particles Seattle in right well. During the course of time, bosons remain self-trapped in the right well.

was formulated by López-Ruiz, Mancini, and Calbet [LRMC95, CGLR02]. In the context of assessing Shannon information entropy, complexity is considered the most efficient measure of how much order and disorder exist in a system [SLS22, MF21]. The SDL and LMC complexity measurements for interacting bosons in the optical lattice are of interest to us. Over the past few years, one of the most difficult problems that has arisen is the implementation of completely controlled quantum many-body systems. Interacting bosons in an external trap at ultracold temperatures enable extraordinary experimental control, making it an ideal test bed for quantum many-body physics research. It has various quantum phases, including superfluid (SF), Mott insulator (MI), and fragmented Mott insulator (FMI). In this chapter, We would like to follow the path from the SF phase to the insulating phase by directly monitoring the change in order, disorder, and complexity. Our main focus is on investigating the transition from the SF phase to the MI phase via the non-monotonic dependency of SDL and LMC complexity on the lattice depth parameter.

We look at a system of $N = 3$ bosons interacting with a contact interaction $\hat{W}(x_i - x_j) = \lambda\delta(x_i - x_j)$ in a one-dimensional three-well optical lattice, and solve the Schrödinger equation given by

$$H = \sum_{i=1}^{N}\left(-\frac{1}{2}\frac{\partial^2}{\partial x^2} + V_{OL}(x_i)\right) + \sum_{i<j}\hat{W}(x_i - x_j) \tag{24}$$

where λ is the strength of the interaction and the bosons are trapped in a lattice of the form $V_{OL}(x) = V_0 sin^2(kx)$. In this work, the lattice depth is changed to get a transition from the SF phase to the MI phase. We use the MCTDHB method to solve the many-body Schrödinger equation with a high level of accuracy. The Shannon information entropy measures, order (Ω), disorder (Δ), and complexity are all part of the general information-theoretical measure. In Fig. 17(a), we plot the many-body Shannon information entropy as a function of lattice depth. For the SF phase, entropy is minimum but not zero. With increase in lattice depth, entropy gradually increases, and at $V_0 = 10.0$, it saturates. With further increase in the lattice depth parameter, entropy remains at its saturation value. Thus, once the MI phase is reached, the system retains that phase even with further increase in lattice depth. In Fig.17(b), Both the order and disorder are plotted against the lattice depth. We find that in the SF state, order is highest and disorder is lowest. The SF state is not fully ordered since neither the order is one nor the disorder is zero. Order decays and disorder grows proportionally when the lattice depth is increased. We interpreted the intersection of the order and disorder plots at $V_0 = 2.8$ as marking the transition from the SF to MI state. At $V_0 = 10.0$, the order becomes exactly zero and the disorder becomes exactly 1.0, confirming that the Mott phase is a random or disorder phase. According to the results of our calculations, the 'SF-MI transition'

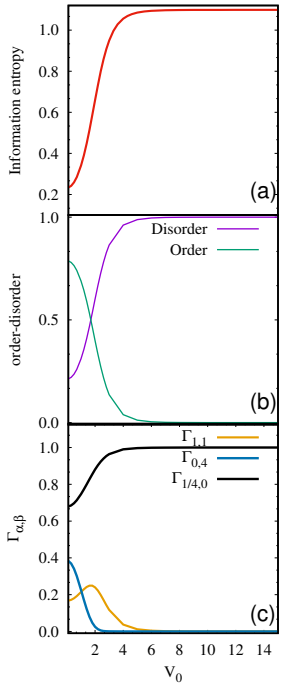

Figure 17: (a) Shannon information entropy (S) plotted against lattice depth (V_0). Entropy is minimum for shallow lattice depth. The transition from SF to MI phase is followed by saturation in the entropy at its maximum value as the lattice depth increases. Order and disorder: During the transition from a superfluid to a mott insulator, order gradually goes from one to zero and disorder gradually goes from zero to one. (c) Plot of Complexity measures ($\Gamma_{\alpha\beta}$) as a function of V_0. $\Gamma_{1/4,0}$, $\Gamma_{1,1}$, $\Gamma_{0,4}$ exhibit type I, type II and type III complexity as discussed in the literature [SDL99]

can be called the 'order-disorder transition'. The SDL complexity $\Gamma_{\alpha\beta}$ is plotted in Fig. 17(c) for various choices of α and β. We find three distinct patterns in the SDL complexity measure for varying combinations of α and β, and we are unable to draw any firm conclusions about which specific combination of these two parameters best characterises complexity. Since complexity is mostly dictated by the disorder Δ for any arbitrary choice of α,β, we observed that the definition given in Eq. 15 is over-universal. As a result, we derive a more insightful complexity, C. We plot the LMC complexity C against the different values of the lattice depth parameter $V0$ in Fig. 18, and we notice that C only evolves in a manner analogous to $\Gamma_{\alpha,\beta}$ when both $\alpha = 1$ and $\beta = 1$. During the transition from the SF phase to the MI phase, this leads one to the conclusion that the bosonic atoms in an optical lattice show type II complexity. None of the other measurements of complexity matter. The distinct maxima in the LMC complexity measure that arises at $V_0 = 3.1$, which is extremely close to the point where order and disorder overlap, is by far the most interesting aspect of this measure. Therefore, given the current value of the system parameter, the precursor point of entry to the Mott phase and escape from the SF phase is situated at $V_0 = 3.1$. The calculation demonstrates that LMC complexity is more thorough and efficient to identify the entry-exit point, which cannot be found using the monotonic rise in SIE. We have also addressed the dynamical measures of SIE and LMC

Table 2: Superfluid to Mott insulator phase transition time dynamics.

Period	**SF state**	**Mott state entry**	**MI phase holding time**	**Mott state exit**	**SF state**
First Cycle	0.0	30.1	23.8	53.9	81.0
Second Cycle	81.0	113.1	24.1	137.2	161.9
Third Cycle	161.9	196.0	23.2	219.2	243.1

complexity. The study is motivated by three factors. (i) How complexity is developed in the system during time evolution. It will practically demonstrate how the system would optimize complexity, which basically will exhibit the ability or inability of the system to self-organize with the external change. (ii) How effective is the dynamical measure of complexity in determining the time-scale of dynamics. (iii) To demonstrate that the dynamical measure of complexity is a more rich predictor than the evolution of SIE. The time-dependence of LMC complexity and Shannon information entropy is calculated and shown in Fig. 19. Our observations are as follow. *(i) For SF phase:*

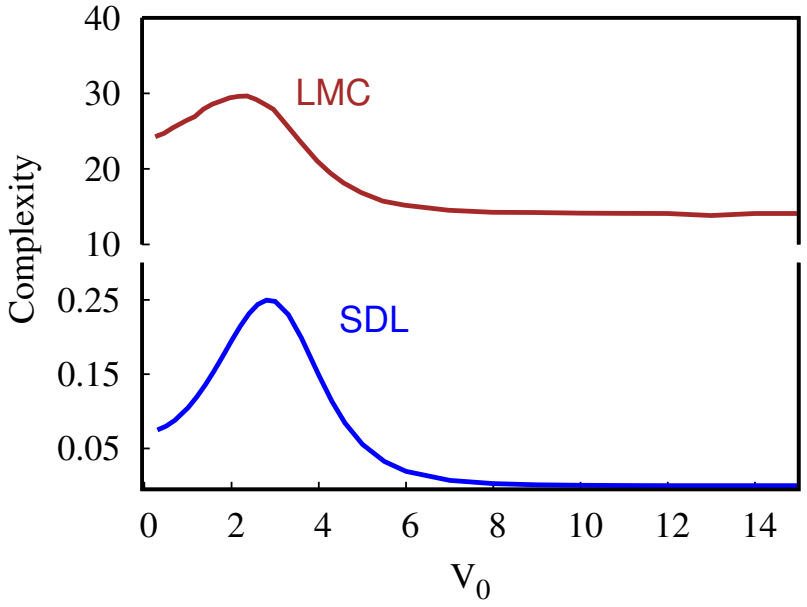

Figure 18: Complexity measures as a function of lattice depth (V_0). The upper graph is for LMC complexity measure and the lower one is for SDL ($\Gamma_{1,1}$) complexity measure. Initially, when the system is in SF phase, complexity has finite value. As V_0 increases, the system becomes more fragmented, and its complexity rises, revealing a maxima. Then, for large V_0, when the system is in MI phase, it saturates to a fixed value. The saturation value is nearly zero for SDL measures and 14.6 for LMC measures. Both LMC and SDL ($\Gamma_{1,1}$) complexity exhibit nearly identical characteristics. The maxima in complexity measure indicates exit from SF phase and entry to MI phase.

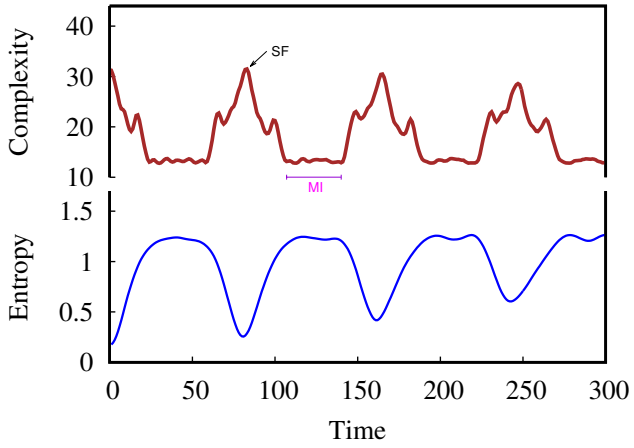

Figure 19: Time evolution of LMC complexity and Shannon information entropy of $N = 3$ bosons in optical lattice as a function of time. Picks in LMC complexity (top) measures quantify the SF phase, and a flat minima signifies the holding time for the system in MI phase. The Shannon information entropy (bottom) exhibits maxima for MI phase and minima for SF phase. The MI state entry time can be determined with more accurately and efficiently using LMC complexity as there is distinct maxima or minima in LMC complexity.

For all cycles, the LMC complexity has unique maxima. Local minima in the entropy represent the same. *(ii) Mott state entry:* LMC complexity has unique minima. The wide peak in the entropy measure represents the Mott state, although the entrance point is not clear. *(iii) Mott Phase:* For all cycles, LMC complexity has a clear plateau on the same time scale as illustrated in Table 2. There is no visible plateau in the associated SIE. There are wide, flat peaks in the first two cycles, but they rapidly decrease in the period commencing. As a result, finding the Mott holding time from the SIE measure is impossible. The time scale is presented in Table 2. *(iv) MI state exit:*In the same time period as in Table 2, the LMC measure shows a rapid rise shortly after the plateau.The corresponding SIE measurement begins to fall, although no discernible change can be reported. We may infer that SIE has qualitative collapse-revival dynamics after the quench. SIE, however, is unable to anticipate any time scale of the dynamical evolution owing to *monotonic* oscillatory behaviour. LMC complexity, on the other hand, has a *distinct* structure that clearly demonstrates the same time-scale of dynamics for all cycles that we have designed from fragmentation. We find that studying the time dynamics of SIE is not a very sensitive tool. In quench dynamics, a rapid rise in lattice depth indicates that we are externally pumping energy into the system, which will be distributed through the Hamiltonian's one-body component. The system may transfer additional energy among interacting bosons and thereby self-organize the external disturbance. However, multiple excited states contribute in a complicated way in long-time dynamics. As a result, the system has a difficult time returning to a perfect SF phase, as seen by the delayed fall in height in the maxima of the LMC measure.

5 Conclusion

The static and dynamics of interacting bosons confined in an optical trap is investigated in detail in this synopsis. MCTDHB method and its efficiency is effectively demonstrated in this summery following a brief introduction. We have defined various information entropies which can be defined to reflect and quantify many-body properties of the ground state of interacting bosons in one-dimensional lattices. These entropies serve the dual purpose to (i) identify phase transitions not seen in the single-particle properties of the system and (ii) allow a connection to known results from random matrix theory. We have also shown that the results obtained from our calculation is well agreement with the results from random matrix theory. Our analysis of the SIE measures is complemented by an analysis of the density and the spatial first- and second-order coherence. We showed that all emergent phases have characteristic density, correlation, and coherence patterns. We hence demonstrated that the superfluid, and the Mott-insulating and the fermionized phases of bosons in one-dimensional lattices are not only characterized uniquely by their densities and Glauber normalized correlation functions.

We have also analyze the relaxation process by the dynamical evolution of the three key quantities, namely the natural occupations, the Shannon information entropy, and the fidelity for small to large interaction strength. We addressed the fundamental question of whether, and on which time-scale, the signatures of the relaxation of the system are seen. For small interaction strength, system does not fully relax. On the other hand, sufficiently large interaction lead the system to a new relaxed state. We have also shown the features of relaxation for an isolated quantum system and its relation to a dynamical quantum phase transition characterized by a collapse point in the quantum fidelity.

For the case of dipolar interacting bosons trapped in double well potential, We investigated Rabi oscillations in the non-interacting limit and self-trapping and finally equilibration dynamics for strong interaction. The calculated average population imbalance qualitatively describes the range of interaction strength to have self-trapping. We observed a very interesting dynamics in the two-body density and established the link between the tunneling dynamics and the role played by the inter-atomic correlation and inter-well coherence. The most subtle dynamical regime is observed at the strong interaction strength when the many-body dynamics exhibits an equilibration dynamics. We observed that for this equilibration dynamics, the many-body state is initially fragmented and then exhibits a plateau structure in the long time dynamics. In complexity work, our motivation is how to consult the various quantum phases with the measure of order-disorder and complexity and also the time scale associated with this. As the lattice depth is an easily controllable parameter experimentally, our theoretical analysis both for the relaxed state as well as dynamically evolve state exhibit that lattice depth can act as order-disorder parameter. SF phase is characterized as an ordered but not properly ordered state, whereas Mott phase is characterized as proper disordered state. Complexity exhibits type II features. SF to MI phase transition can be renamed as "order-disorder" transition. In the quench dynamics, we observe the collapse revival feature qualitatively in all statistical measures. We also able to present the time scale of different phases through several cycles. Additionally, we observe that oscillations in the dynamics of the LMC complexity measure for incommensurate filling clearly demonstrate that the transition from superfluid to Mott-insulator is incomplete. Overall, we find that different complexity structure makes it more sensitive than the traditional application of Shannon information entropy.

References

[AA08] JC Angulo and J Antolín. Atomic complexity measures in position and momentum spaces. *The Journal of chemical physics*, 128(16):164109, 2008.

[AAG+05] Th. Anker, M. Albiez, R. Gati, S. Hunsmann, B. Eiermann, A. Trombettoni, and M. K. Oberthaler. Nonlinear self-trapping of matter waves in periodic potentials. *Phys. Rev. Lett.*, 94:020403, Jan 2005.

[AC00] C. Adami and N.J. Cerf. Physical complexity of symbolic sequences. *Physica D: Nonlinear Phenomena*, 137(1):62–69, 2000.

[AEM+95] M. H. Anderson, J. R. Ensher, M. R. Matthews, C. E. Wieman, and E. A. Cornell. Observation of bose-einstein condensation in a dilute atomic vapor. *Science*, 269(5221):198–201, 1995.

[AGF+05] Michael Albiez, Rudolf Gati, Jonas Fölling, Stefan Hunsmann, Matteo Cristiani, and Markus K. Oberthaler. Direct observation of tunneling and nonlinear self-trapping in a single bosonic josephson junction. *Phys. Rev. Lett.*, 95:010402, Jun 2005.

[ASC07] Ofir E. Alon, Alexej I. Streltsov, and Lorenz S. Cederbaum. Unified view on multiconfigurational time propagation for systems consisting of identical particles. *The Journal of Chemical Physics*, 127(15):154103, 2007.

[ASC08] Ofir E. Alon, Alexej I. Streltsov, and Lorenz S. Cederbaum. Multiconfigurational time-dependent hartree method for bosons: Many-body dynamics of bosonic systems. *Phys. Rev. A*, 77:033613, Mar 2008.

[Ast19] Sergey A. Astashkevich. Comparison of information-theoretic products and inequalities for the lowest bound and unbound electronic states of h2+ based on exact calculation. *Physics Letters A*, 383(24):2854–2861, 2019.

[Bos24] S. N. Bose. Plancks gesetz und lichtquantenhypothese. *Zeitschrift für Physik*, 26:178, 1924.

[BSA+18] A. Burchianti, F. Scazza, A. Amico, G. Valtolina, J. A. Seman, C. Fort, M. Zaccanti, M. Inguscio, and G. Roati. Connecting dissipation and phase slips in a josephson junction between fermionic superfluids. *Phys. Rev. Lett.*, 120:025302, Jan 2018.

[BSTH95] C. C. Bradley, C. A. Sackett, J. J. Tollett, and R. G. Hulet. Evidence of bose-einstein condensation in an atomic gas with attractive interactions. *Phys. Rev. Lett.*, 75:1687–1690, Aug 1995.

[CBZP92] J. I. Cirac, R. Blatt, P. Zoller, and W. D. Phillips. Laser cooling of trapped ions in a standing wave. *Phys. Rev. A*, 46:2668–2681, Sep 1992.

[CCP04] M.M. Cerimele, M.L. Chiofalo, and F. Pistella. From coherent to incoherent dynamical behaviour of quantum atomic gases in periodic potentials. *Applied Numerical Mathematics*, 49(3):319–330, 2004. Applied Scientific Computing - Grid Generation, Approximated Solutions and Visualization.

[CDJ+04] T. Calarco, U. Dorner, P. S. Julienne, C. J. Williams, and P. Zoller. Quantum computations with atoms in optical lattices: Marker qubits and molecular interactions. *Phys. Rev. A*, 70:012306, Jul 2004.

[CGJT10] Cheng Chin, Rudolf Grimm, Paul Julienne, and Eite Tiesinga. Feshbach resonances in ultracold gases. *Rev. Mod. Phys.*, 82:1225–1286, Apr 2010.

[CGLR02] Raquel G. Catalán, José Garay, and Ricardo López-Ruiz. Features of the extension of a statistical measure of complexity to continuous systems. *Phys. Rev. E*, 66:011102, Jul 2002.

[CMP05] K Ch Chatzisavvas, Ch C Moustakidis, and CP Panos. Information entropy, information distances, and complexity in atoms. *The Journal of chemical physics*, 123(17):174111, 2005.

[DMA+95] K. B. Davis, M. O. Mewes, M. R. Andrews, N. J. van Druten, D. S. Durfee, D. M. Kurn, and W. Ketterle. Bose-einstein condensation in a gas of sodium atoms. *Phys. Rev. Lett.*, 75:3969–3973, Nov 1995.

[DMJ+95] Kendall B. Davis, Marc-Oliver Mewes, Michael A. Joffe, Michael R. Andrews, and Wolfgang Ketterle. Evaporative cooling of sodium atoms. *Phys. Rev. Lett.*, 74:5202–5205, Jun 1995.

[Ein25] A. Einstein. Zur quantentheorie des idealen gases. *Sitzungsberichte der Preußischen Akademie der Wissenschaften*, 3, Oct 1925.

[GBM+01] Markus Greiner, Immanuel Bloch, Olaf Mandel, Theodor W. Hänsch, and Tilman Esslinger. Exploring phase coherence in a 2d lattice of bose-einstein condensates. *Phys. Rev. Lett.*, 87:160405, Oct 2001.

[GME+02a] Markus Greiner, Olaf Mandel, Tilman Esslinger, Theodor W. Hänsch, and Immanuel Bloch. Quantum phase transition from a superfluid to a mott insulator in a gas of ultracold atoms. *Nature*, 415(6867):39–44, Jan 2002.

[GME+02b] Markus Greiner, Olaf Mandel, Tilman Esslinger, Theodor W. Hänsch, and Immanuel Bloch. Quantum phase transition from a superfluid to a mott insulator in a gas of ultracold atoms. *Nature*, 415(6867):39–44, Jan 2002.

[GVL+01] A. Görlitz, J. M. Vogels, A. E. Leanhardt, C. Raman, T. L. Gustavson, J. R. Abo-Shaeer, A. P. Chikkatur, S. Gupta, S. Inouye, T. Rosenband, and W. Ketterle. Realization of bose-einstein condensates in lower dimensions. *Phys. Rev. Lett.*, 87:130402, Sep 2001.

[GWH+05] Axel Griesmaier, Jörg Werner, Sven Hensler, Jürgen Stuhler, and Tilman Pfau. Bose-einstein condensation of chromium. *Phys. Rev. Lett.*, 94:160401, Apr 2005.

[Hal81] F. D. M. Haldane. Effective harmonic-fluid approach to low-energy properties of one-dimensional quantum fluids. *Phys. Rev. Lett.*, 47:1840–1843, Dec 1981.

[HGM+09] Elmar Haller, Mattias Gustavsson, Manfred J Mark, Johann G Danzl, Russell Hart, Guido Pupillo, and Hanns-Christoph Nägerl. Realization of an excited, strongly correlated quantum gas phase. *Science (New York, N.Y.)*, 325(5945):1224—1227, September 2009.

[HHM+10] E. Haller, R. Hart, M. J. Mark, J. G. Danzl, L. Reichs"ollner, M. Gustavsson, M. Dalmonte, G. Pupillo, and H.-C. N"agerl. Pinning quantum phase transition for a luttinger liquid of strongly interacting bosons. *Nature*, 466(7306):597–600, Jul 2010.

[HRMB09] K Henderson, C Ryu, C MacCormick, and M G Boshier. Experimental demonstration of painting arbitrary and dynamic potentials for bose–einstein condensates. *New Journal of Physics*, 11(4):043030, apr 2009.

[HS75] T. W. Hansch and A. L. Schawlow. Cooling of gases by laser radiation. *Optics Communications*, 13(1):68–69, January 1975.

[Hua13] Yichen Huang. Entanglement detection: complexity and shannon entropic criteria. *Ieee transactions on information theory*, 59(10):6774–6778, 2013.

[JBC+98] D. Jaksch, C. Bruder, J. I. Cirac, C. W. Gardiner, and P. Zoller. Cold bosonic atoms in optical lattices. *Phys. Rev. Lett.*, 81:3108–3111, Oct 1998.

[KPP+20] W. J. Kwon, G. Del Pace, R. Panza, M. Inguscio, W. Zwerger, M. Zaccanti, F. Scazza, and G. Roati. Strongly correlated superfluid order parameters from dc josephson supercurrents. *Science*, 369(6499):84–88, 2020.

[KS81] Peter Kramer and Marcos Saraceno. *Geometry of the Time-Dependent Variational Principle in Quantum Mechanics*. Springer Berlin, Heidelberg, 1981.

[Kva13] Simen Kvaal. Variational formulations of the coupled-cluster method in quantum chemistry. *Molecular Physics*, 111(9-11):1100–1108, 2013.

[KWW04a] Toshiya Kinoshita, Trevor Wenger, and David S. Weiss. Observation of a one-dimensional tonks-girardeau gas. *Science*, 305(5687):1125–1128, 2004.

[KWW04b] Toshiya Kinoshita, Trevor Wenger, and David S. Weiss. Observation of a one-dimensional tonks-girardeau gas. *Science*, 305(5687):1125–1128, 2004.

[LB16] Axel U. J. Lode and Christoph Bruder. Dynamics of hubbard hamiltonians with the multiconfigurational time-dependent hartree method for indistinguishable particles. *Phys. Rev. A*, 94:013616, Jul 2016.

[LBYL11] Mingwu Lu, Nathaniel Q. Burdick, Seo Ho Youn, and Benjamin L. Lev. Strongly dipolar bose-einstein condensate of dysprosium. *Phys. Rev. Lett.*, 107:190401, Oct 2011.

[LCK15] Axel U. J. Lode, Barnali Chakrabarti, and Venkata K. B. Kota. Many-body entropies, correlations, and emergence of statistical relaxation in interaction quench dynamics of ultracold bosons. *Phys. Rev. A*, 92:033622, Sep 2015.

[LGK+21] Rui Lin, Christoph Georges, Jens Klinder, Paolo Molignini, Miriam Büttner, Axel U. J. Lode, R. Chitra, Andreas Hemmerich, and Hans Keßler. Mott transition in a cavity-boson system: A quantitative comparison between theory and experiment. *SciPost Phys.*, 11:30, 2021.

[LIB+10] Oren Lahav, Amir Itah, Alex Blumkin, Carmit Gordon, Shahar Rinott, Alona Zayats, and Jeff Steinhauer. Realization of a sonic black hole analog in a bose-einstein condensate. *Phys. Rev. Lett.*, 105:240401, Dec 2010.

[LLM+20] Axel U. J. Lode, Camille Lévêque, Lars Bojer Madsen, Alexej I. Streltsov, and Ofir E. Alon. Colloquium: Multiconfigurational time-dependent hartree approaches for indistinguishable particles. *Rev. Mod. Phys.*, 92:011001, Feb 2020.

[LMP+20] Rui Lin, Paolo Molignini, Luca Papariello, Marios C Tsatsos, Camille Lévêque, Storm E Weiner, Elke Fasshauer, R Chitra, and Axel U J Lode. MCTDH-x: The multiconfigurational time-dependent hartree method for indistinguishable particles software. *Quantum Science and Technology*, 5(2):024004, mar 2020.

[Lod16] Axel U. J. Lode. Multiconfigurational time-dependent hartree method for bosons with internal degrees of freedom: Theory and composite fragmentation of multicomponent bose-einstein condensates. *Phys. Rev. A*, 93:063601, Jun 2016.

[LR05] Ricardo López-Ruiz. Shannon information, lmc complexity and rényi entropies: a straightforward approach. *Biophysical chemistry*, 115(2-3):215–218, 2005.

[LRMC95] R. López-Ruiz, H.L. Mancini, and X. Calbet. A statistical measure of complexity. *Physics Letters A*, 209(5):321–326, 1995.

[LSA+12] Axel U. J. Lode, Kaspar Sakmann, Ofir E. Alon, Lorenz S. Cederbaum, and Alexej I. Streltsov. Numerically exact quantum dynamics of bosons with time-dependent interactions of harmonic type. *Phys. Rev. A*, 86:063606, Dec 2012.

[LSB+20] Niclas Luick, Lennart Sobirey, Markus Bohlen, Vijay Pal Singh, Ludwig Mathey, Thomas Lompe, and Henning Moritz. An ideal josephson junction in an ultracold two-dimensional fermi gas. *Science*, 369(6499):89–91, 2020.

[MF21] César Martínez-Flores. Shannon entropy and fisher information for endohedral confined one- and two-electron atoms. *Physics Letters A*, 386:126988, 2021.

[MO06] Oliver Morsch and Markus Oberthaler. Dynamics of bose-einstein condensates in optical lattices. *Rev. Mod. Phys.*, 78:179–215, Feb 2006.

[NMCW95] N. R. Newbury, C. J. Myatt, E. A. Cornell, and C. E. Wieman. Gravitational sisyphus cooling of ^{87}Rb in a magnetic trap. *Phys. Rev. Lett.*, 74:2196–2199, Mar 1995.

[NSR18] Elettra Neri, Francesco Scazza, and Giacomo Roati. Coherent and dissipative transport in a josephson junction between fermionic superfluids of 6li atoms. *AIP Conference Proceedings*, 1950(1):020003, 2018.

[NTL+19] J. H. V. Nguyen, M. C. Tsatsos, D. Luo, A. U. J. Lode, G. D. Telles, V. S. Bagnato, and R. G. Hulet. Parametric excitation of a bose-einstein condensate: From faraday waves to granulation. *Phys. Rev. X*, 9:011052, Mar 2019.

[Pau40] W. Pauli. The connection between spin and statistics. *Phys. Rev.*, 58:716–722, Oct 1940.

[PCMK07] C.P. Panos, K.Ch. Chatzisavvas, Ch.C. Moustakidis, and E.G. Kyrkou. Comparison of sdl and lmc measures of complexity: Atoms as a testbed. *Physics Letters A*, 363(1):78–83, 2007.

[PO56] Oliver Penrose and Lars Onsager. Bose-einstein condensation and liquid helium. *Phys. Rev.*, 104:576–584, Nov 1956.

[RCT22] Rhombik Roy, Barnali Chakrabarti, and Andrea Trombettoni. Quantum dynamics of few dipolar bosons in a double-well potential. *European Physical Journal D*, 76(24):215303, feb 2022.

[RGT+18] R. Roy, A. Gammal, M. C. Tsatsos, B. Chatterjee, B. Chakrabarti, and A. U. J. Lode. Phases, many-body entropy measures, and coherence of interacting bosons in optical lattices. *Phys. Rev. A*, 97:043625, Apr 2018.

[RLL+19] Rhombik Roy, Camille Lévêque, Axel U. J. Lode, Arnaldo Gammal, and Barnali Chakrabarti. Fidelity and entropy production in quench dynamics of interacting bosons in an optical lattice. *Quantum Reports*, 1(2):304–316, 2019.

[SAC07] Alexej I. Streltsov, Ofir E. Alon, and Lorenz S. Cederbaum. Role of excited states in the splitting of a trapped interacting bose-einstein condensate by a time-dependent barrier. *Phys. Rev. Lett.*, 99:030402, Jul 2007.

[SB97] C. V. Sukumar and D. M. Brink. Spin-flip transitions in a magnetic trap. *Phys. Rev. A*, 56:2451–2454, Sep 1997.

[SDL99] J. S. Shiner, Matt Davison, and P. T. Landsberg. Simple measure for complexity. *Phys. Rev. E*, 59:1459–1464, Feb 1999.

[Sen11] Kali Das Sen. *Statistical complexity: applications in electronic structure*. Springer Science & Business Media, 2011.

[SFGS97] A. Smerzi, S. Fantoni, S. Giovanazzi, and S. R. Shenoy. Quantum coherent atomic tunneling between two trapped bose-einstein condensates. *Phys. Rev. Lett.*, 79:4950–4953, Dec 1997.

[SKC+01] F. Schreck, L. Khaykovich, K. L. Corwin, G. Ferrari, T. Bourdel, J. Cubizolles, and C. Salomon. Quasipure bose-einstein condensate immersed in a fermi sea. *Phys. Rev. Lett.*, 87:080403, Aug 2001.

[SKH+06] T. Schumm, P. Krüger, S. Hofferberth, I. Lesanovsky, S. Wildermuth, S. Groth, I. Bar-Joseph, L. M. Andersson, and J. Schmiedmayer. A double well interferometer on an atom chip. *Quantum Information Processing*, 5(6):537–558, Dec 2006.

[SLR05] Juan R. Sánchez and Ricardo López-Ruiz. A method to discern complexity in two-dimensional patterns generated by coupled map lattices. *Physica A: Statistical Mechanics and its Applications*, 355(2):633–640, 2005.

[SLS22] S. J. C. Salazar, H. G. Laguna, and R. P. Sagar. Pairwise and higher-order statistical correlations in excited states of quantum oscillator systems. *Eur. Phys. J Plus*, 137:19, Oct 2022.

[TSMRD16] Irene V Toranzo, Pablo Sánchez-Moreno, Łukasz Rudnicki, and Jesús S Dehesa. One-parameter fisher–rényi complexity: notion and hydrogenic applications. *Entropy*, 19(1):16, 2016.